Ecosystems (2025) 28:39
https://doi.org/10.1007/s10021-025-00974-9

© 2025 The Author(s)

ORIGINAL ARTICLE

The Structural and Functional Impacts of Invasive *Psidium cattleianum* in Forests on the Island of Hawai'i

Tara Seely,[1]* Lucas Berio Fortini,[2] Yutong Liang,[3] and John Battles[1]

[1]*Department of Environmental Science, Policy, and Management, University of California, 130 Mulford Hall #3114, Berkeley, California 94720-3114, USA;* [2]*U.S. Geological Survey, Pacific Island Ecosystems Research Center, P.O. Box 44, Hawaii National Park, Hawaii 96718, USA;* [3]*Sustainable Energy and Environment Thrust, The Hong Kong University of Science and Technology (Guangzhou), Guangzhou 511453, Guangdong, China*

Abstract

During the past century, the proliferation of invasive species has contributed to loss of biodiversity and ecosystem degradation. In forests, invasive tree species can alter ecosystem function, but the underlying mechanisms of these changes are not fully understood. We use the ongoing invasion of *P. cattleianum* on the Island of Hawai'i to test the hypotheses that invasive structural changes drive changes to forest evapotranspiration (ET). The aim of our study is first to quantify the structural changes to native 'ōhi'a -dominated forest impacted by a gradient of *P. cattleianum* invasion. Our results suggest that invasive *P. cattleianum* causes significant changes to the vegetation density and structure of native forest on the Island of Hawai'i, including increased vegetation area index, decreased mean leaf height, and decreased structural heterogeneity. Second, we strove to understand the functional implications of structural changes through a biophysical modeling simulation, testing the sensitivity of ET to canopy structure under contrasting scenarios. Modeling the functional impact of structural change, we found that plots with *P. cattleianum* invasion importance value (IV_{inv}) above 0.35 have a higher likelihood to increase ET compared to plots with *P. cattleianum* invasion less than 0.35 IV_{inv}. Modeled increases in ET due to invasion ranged from 19 and 123% relative to native transects. The large variation in ET increases is caused by structural variation because the modeling scenarios did not include potential species differences in leaf physiology. Diagnostic scenario modeling shows the effect size of increased leaf area on modeled ET is constrained by the structural arrangement, that is vertical distribution, of the increased vegetation. Thus, invasion structure that increases vegetation density in taller, more sunlit forest strata will lead to a greater increase in ET compared to invasion structure that increases vegetation density in the shaded forest understory. Overall, we conclude the vertical distribution of vegetation is an important factor shaping the impact of invasive *P. cattleianum* on the forest water balance.

Received 25 March 2024; accepted 4 March 2025;
published online 7 July 2025

Supplementary Information: The online version contains supplementary material available at https://doi.org/10.1007/s10021-025-00974-9.

Author Contributions: Tara Seely designed and carried out the study, analysis, and writing. Lucas Berio Fortini helped with study design, structure, and editing. Yutong Liang helped with modeling. John Battles helped with study design, structure, and editing.

**Corresponding author; e-mail:* tara_seely@berkeley.edu

Key words: Invasive species; Evapotranspiration; Ecohydrology; Ecosystem science; Forest structure; Ecosystem function; Terrestrial LiDAR; Biophysical model.

Highlights

- Invasive tree *P. cattleianum* changes structure and density of forest vegetation.
- Changes in vegetation may cause forest to release more water into the atmosphere.
- Invasive foliage in the upper canopy uses more water compared to the understory.

Introduction

In the past century, the global, accelerating spread of invasive species has contributed to biodiversity loss and ecosystem degradation (McGeoch and others 2010; Pyšek and Richardson 2010; Seebens and others 2017). One of the most concerning effects of invasive species is their disruption to ecosystem function. In the case of invasive plants, invasion can alter the nutrient cycling, primary productivity, and hydrology of ecosystems. However, the nature of these effects depends on the invasive species' functional traits and morphology (Pejchar and Mooney 2009; Ehrenfeld 2010; Vilà and others 2011). Species-specific variation and methodological limitations make the impacts of invasive plants on ecosystem function challenging to assess and hard to predict (Calder and Dye 2001; Cavaleri and Sack 2010; Vilà and others 2011). Developing approaches to measure invasive traits and link them to changes in ecosystem function via modeling is paramount to addressing this global threat (Ehrenfeld 2010).

This study addresses the functional impact of invasive species on evapotranspiration (ET), an ecohydrologic process. In many cases, invasive plants jeopardize water resources by transpiring more compared to native vegetation (Calder and Dye 2001; Pejchar and Mooney 2009). However, the extent of such functional impacts appears to be species- and ecosystem-dependent. Understanding the effect of invasive plants on ET requires in-situ measurements or a combination of measurements and validated modeling. Modeling forest ET has challenges; forest-atmosphere fluxes depend on a host of interacting conditions, both physical (for example, climate and soil) and biological (for example, leaf-level gas exchange and leaf area) (Calder and Dye 2001; Cavaleri and Sack 2010). The complexity of modeling ET is exemplified by disconnects in water use across different scales, that is, individual tree water use does not scale up to forest-wide water budgets (Cavaleri and Sack 2010). Therefore, species function other than physiological water use need to be explored for their impact on ET. Such assessments help broaden our understanding of the impact of invasive species on ecosystem ecohydrology. Our study addresses these challenges (1) conceptually, by exploring forest structure as an understudied functional component of ecosystems influencing changes to ET and (2) methodologically, by incorporating empirical measurements of structural complexity into an ET model (Bonan 2019).

Conceptually, our work posits structure as a functional component which scales invasive plant water use to stand-level ET. Structure refers to the three-dimensional spatial arrangement of stems and leaves. Although total leaf density is an essential ecological trait, canopy structure plays a key, independent role in ecosystem state changes and mediating carbon, water, and energy fluxes (Stark and others 2020; Béland and Baldocchi 2021; Frenne and others 2021). Despite structure's importance, structural attributes are infrequently directly measured. Additionally, the relationships between structural features and forest-atmosphere interactions are complex (Stark and others 2020; Murphy and others 2022). Therefore, it is important to quantify change in forest structure due to species invasion and understand the functional implications this change has on forest ET.

Methodologically, light detection and ranging (LiDAR) substantially improves the ability to measure structure and parameterize complex biophysical models (Béland and others 2019). Terrestrial laser scanning (TLS) deploys LiDAR beneath the forest canopy, yielding high resolution, detailed models of the forest. TLS data can be used to estimate vertical arrangement of vegetation density. The detail provided by the TLS method exceeds that of more conventional methods to measure structure. For example, a conventional estimate of vegetative surface area – basal area – reports the area occupied by tree stems at 1.37 m height. Another, based on measurements of light attenuation at the ground level, measures leaf area per unit ground area (that is, leaf area index, LAI) for a column of vegetation (Buckley and others 1999). These spatially integrated measurements are well suited to parameterize conventional ''big leaf'' biophysical models, which estimate ET by simpli-

fying the forest into a single, functionally homogenous unit. In comparison, multilayer biophysical models require spatially explicit forest parameters to approximate forest-atmosphere fluxes. Multilayer canopy models, which incorporate forest structure (vertical leaf arrangement) in addition to LAI, produce more accurate predictions of water and carbon fluxes compared to the big leaf model (Bonan and others 2021). Thus, TLS measurements allow the integration of structural complexity (that is, functional trait) into multilayer models estimating ET (that is, impact to ecosystem function).

Island systems are particularly vulnerable to ecosystem change driven by invasive species. For example, Pyšek and others (2012) found island systems in contrast to continents displayed a greater decrease in species richness due to invasive plants. Not all ecosystems experience a decrease in species richness after invasion, but in tropical islands, the combination of frequent introductions and available niche space due to disharmonic flora increase the likelihood invasive plants will establish and spread (Denslow 2003; Kleunen and others 2015; König and others 2021; Rojas-Sandoval and others 2022). Second, ecosystem functioning on islands tends to be more sensitive to disruption by invasive species (Reaser and others 2007). For example, the introduction of fire-facilitated invasive grasses to the Island of Hawai'i has increased the frequency and intensity of fire, resulting in a positive feedback cycle between fire and invasive species spread (D'Antonio and Vitousek 1992). Similarly, invasive nitrogen-fixing trees change nutrient dynamics and tree growth rates (Vitousek and others 1987). Invasive species are also linked to disruptions in the hydrologic cycle (Strauch and others 2017). Invasive plant removal experiments show stand-level evapotranspiration (ET) significantly decreases in the absence of invasive trees (Cavaleri and others 2014). These latter hydrologic effects of invasive species are concerning because isolated islands are dependent on finite freshwater resources (Giambelluca 2002; Safeeq and Fares 2012).

We use the widespread, ongoing invasion of *Psidium cattleianum* (strawberry guava) on the Island of Hawai'i to test hypotheses about the impact of canopy structure on ET. *P. cattleianum* converts open-canopy native forests previously dominated by *Metrosideros polymorpha* ('ōhi'a) into dense, short-stature thickets (Asner and others 2008; Strauch and others 2017). *P. cattleianum* is referred to as ''water demanding'' and causes decreased, flashier streamflow in invaded watersheds (Takahashi and others 2011; Strauch and others 2017). *P. cattleianum* has the capacity to alter hydrology, but much *P. cattleianum* research has emphasized infiltration and throughfall rather than species functional traits (Mair and Fares 2010; Strauch and others 2017; Fortini and others 2020). Functionally, carbon isotope data indicate *P. cattleianum* uses water inefficiently, but no significant differences in leaf-level gas exchange between *P. cattleianum* and *M. polymorpha* have been confirmed (Ostertag and others 2009; Giambelluca 2016). One study documenting differences in ET in native and invaded sites showed a 29% increase in LAI due to invasion only led to a 6% increase in ET (Giambelluca 2016). The evidence suggests the impacts of *P. cattleianum* on the water cycle are driven by more than plant physiology and amount of leaf material. Thus *P. cattleianum* invasion offers a scenario to investigate the role of structure as a driver of eco-hydrologic change.

The first aim of our study is to characterize and quantify the structural changes to native 'ōhi'a-dominated forest caused by a gradient of *P. cattleianum* invasion. Second, we strove to understand the functional implications of invasive-driven structural changes. Namely, we incorporated empirically measured forest structure into a multilayer biophysical model to estimate forest ET. Finally, we used these analytical results to design hypothetical model simulations which tested the sensitivity of ET to contrasting scenarios of canopy structure. Research questions aligned with each of the three study components include: 1) How does *P. cattleianum* invasion change forest structure? 2) How do invasive-driven structural changes functionally affect ET? 3) Does the structural arrangement of *P. cattleianum* affect ET independent of total vegetation density and species composition?

Methods

Study Sites

In December 2020 and January 2021, we sampled five sites in montane and submontane, mesic, and wet forests of the Island of Hawai'i (Figure 1). Study sites spanned elevation and climate gradients within *M. polymorpha*'s range to capture site variability (Adee and Conrad 1990; Table 1). Sites were located on the windward side of the Island of Hawai'i because the wetter climate provides favorable conditions for *P. cattleianum* invasion (Strauch and others 2017). Within each site, three transects spanned the site's range of *P. cattleianum* invasion. We differentiated the three transects based on the

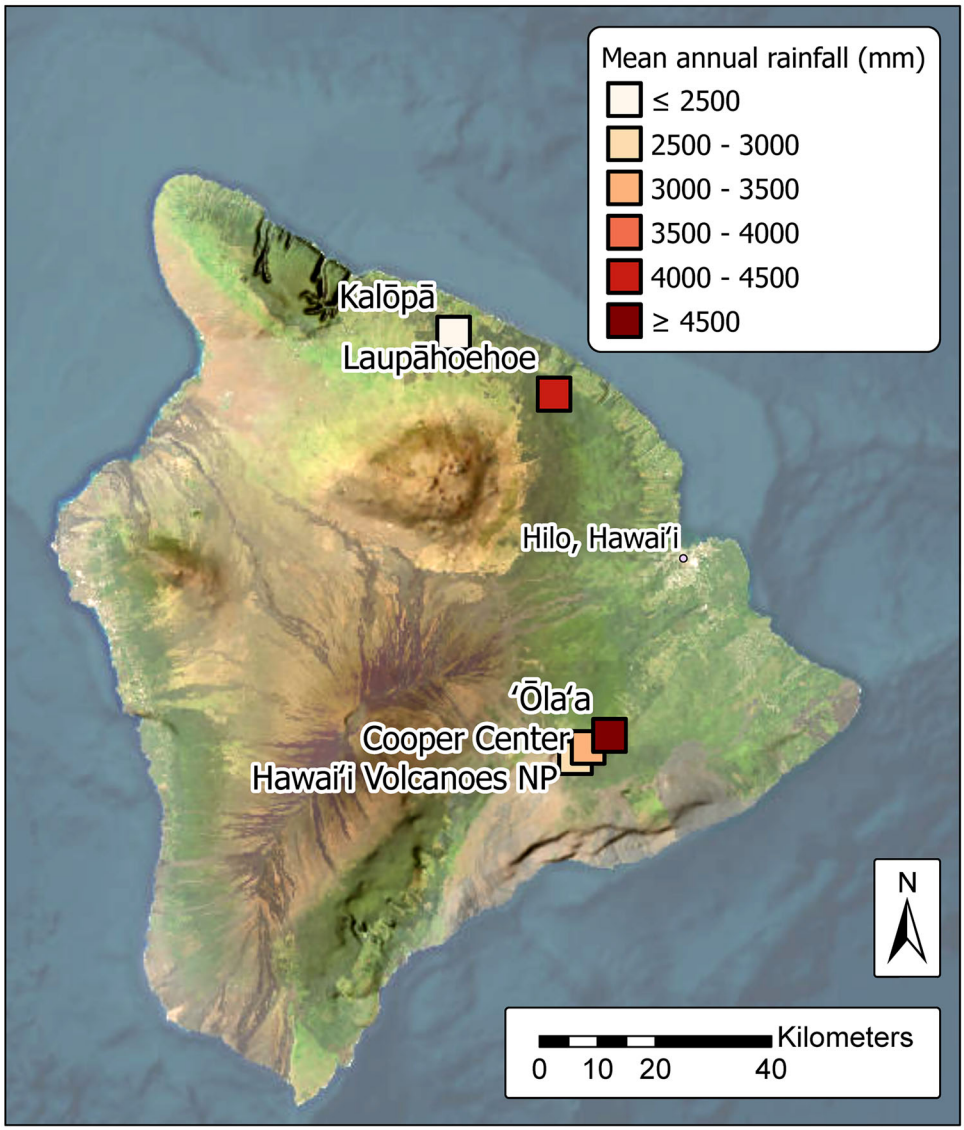


Figure 1. Map of study sites sampled on the windward side of the Island of Hawai'i across a gradient of mean annual rainfall (Esri and others 2025). Additional site information is provided in Table 1.

relative dominance of native versus invasive tree species: native species most dominant, that is ''native''; shared dominance between native and invasive species, that is ''mixed''; or invasive species most dominant, that is ''invasive.'' Transects were 40 m X 10 m. To ensure relatively consistent forest composition, transects sometimes contained an angle or were broken into two distinct segments, but the total area sampled was consistently 400 m^2.

Field Measurements

At 13 points spaced over the 40 m X 10 m transect, species-specific basal area was measured using a basal area prism (BAF = 5), which is a variable-radius sampling technique widely used in forest inventory methods (Wensel and others 1980; Becker and Nichols 2011; Supp. S4; Figure 2). At each point, canopy species intercept was recorded (Bonham 2013; Supp. S2; Figure 2); canopy species present for ≥ 4 points in a transect were considered a dominant species (Table 1).

Terrestrial Laser Scanning (TLS)

Terrestrial laser scanning (TLS) using a Leica BLK360 (Leica Geosystems, Heerbrugg, Switzerland) produced a point cloud of each transect cropped to a total area of 40 m X 6 m and thinned to a point density of 1 per 0.1 m^3 (Supp. S5). The point cloud was created from multiple scans spaced approximately 2.5 m apart, registered, or stitched,

Table 1. Elevation, Climate, Substrate, and Canopy Species of Study Sites on the Windward Side of the Island of Hawai'i

Site	Elevation range (m)	Mean annual rainfall (mm)	Mean annual noon temperature (°C)	Substrate		Dominant canopy species
				Stratum	Age (yr)	
Kalōpā	579–629	2467 ± 90	21.6 ± 1.6	Hāmākua Volcanics	64,000–300,000	*A. angustifolia; M. polymorpha; P. cattleianum*
Laupāhoehoe	763–1053	4015 ± 131	18.7 ± 1.4	Laupāhoehoe Volcanics	5,000–11,000	*M. polymorpha; P. cattleianum*
'Ōla'a	804–935	5129 ± 155	18.8 ± 1.2	Puna Basalt	400–750	*M. polymorpha; P. cattleianum*
Cooper Center	1116–1122	3290 ± 153	17.8 ± 1.3	Puna Basalt	400–750	*M. polymorpha; P. cattleianum*
Hawai'i Volcanoes NP	1121–1202	2556 ± 148	17.9 ± 1.5	Puna Basalt	560–620	*M. polymorpha; M. faya; P. cattleianum*

'NP' indicates National Park. Species include Araucaria angustifolia, Metrosideros polymorpha, Morella faya, and Psidium cattleianum (Giambelluca and others 2013, 2014; U.S. Geological Survey (USGS) 2015; Hawaii statewide GIS program 2021; Sherrod and others 2021).

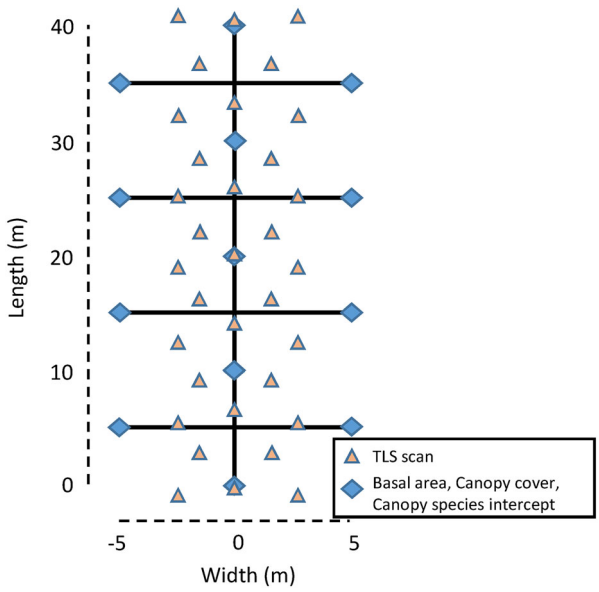


Figure 2. Schematic of field sampling design.

together in Recap Pro (Figure 2). The instrument had 10-mm point spacing at 10 m and full angle beam divergence of 0.4 mrad. The Leica BLK360 collected photographs with each scan which assisted with point cloud registration and tree density estimation. Point clouds were normalized, thinned, and voxelized in R (Supp. S5). The normalized point density in each 1 m^3 voxel was used to calculate vegetation area index (VAI), a dimensionless metric defined by Atkins and others (2018) that represents vegetative density ranging from 0 to 10 (Figure 3). TLS-derived VAI is not an analogous measurement to LAI but is used as a proxy for LAI when appropriately scaled (Almeida and others 2019). The R package *forestR* was used to extract canopy structural measurements from TLS-derived VAI estimates (Atkins and others 2018).

Invasion Gradient

The extent of *P. cattleianum* invasion, or invasion gradient, was quantified by the invasion importance value (IV_{inv}). The IV_{inv} for each transect was calculated using averaged basal area and tree density estimates, the latter of which was calculated using a point-quarter method with data derived from the Leica BLK360 photographs (Supp. S4). Field-based measurement data were not available for site Kalōpā; therefore, basal area was measured using the point cloud.

We expressed the *P. cattleianum* invasion importance value (IV_{inv}) at each site:

$$IV_{inv} = (\text{rel den}_{inv} + \text{rel ba}_{inv}) \div 2 \quad (1)$$

where IV_{inv} is the invasion importance value, rel den_{inv} is the relative tree density of *P. cattleianum*, and rel ba_{inv} is the relative basal area of *P. cattleianum* (Eq. 1).

Density and Structural Metrics

Vegetative density was summarized for each transect with Total VAI, the transect mean of the sum of VAI for a column of forest per square meter area (Atkins and others 2018, Figure 3). Then, four

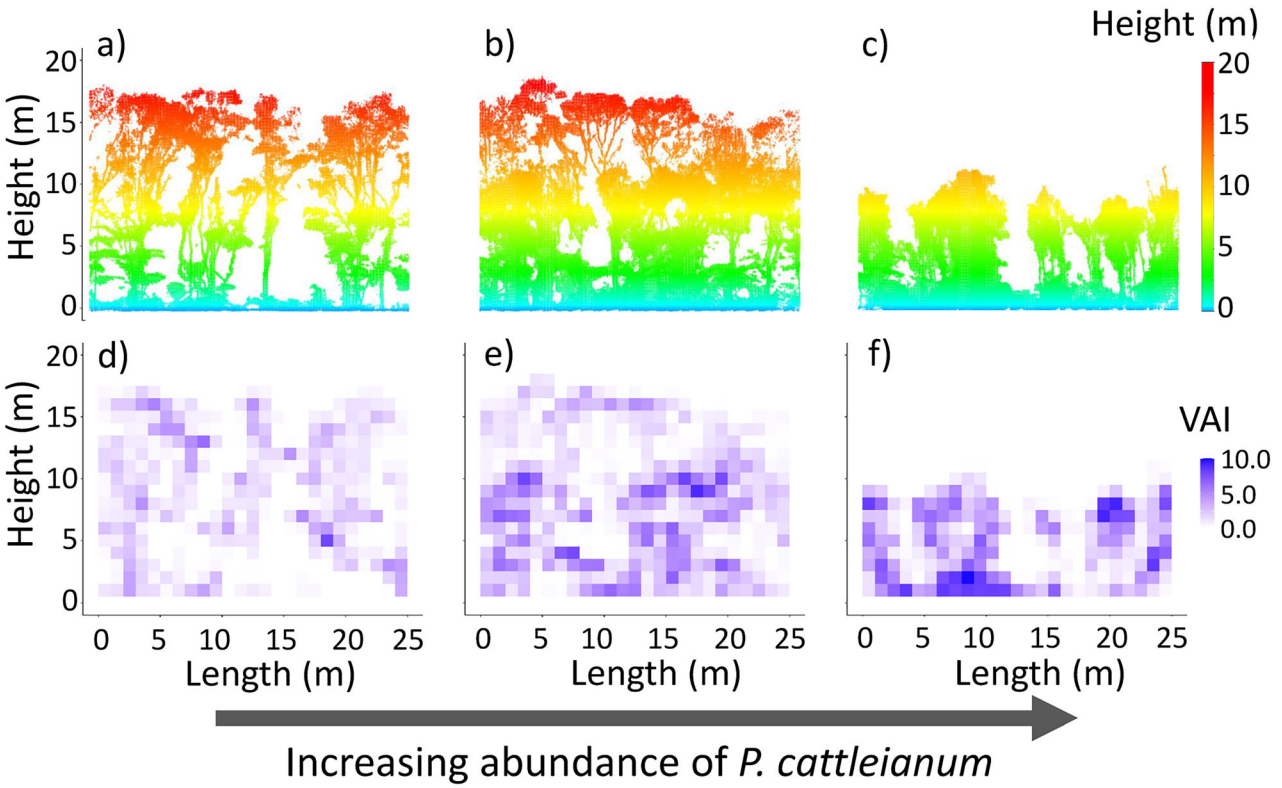


Figure 3. Cross-sections from point clouds of forest structure, 25 m in length and 1 m in depth, derived from terrestrial laser scanning (TLS) for **a** low abundance, **b** moderate abundance, and **c** high abundance of *P. cattleianum*. The corresponding distribution of vegetation area index (VAI) is shown for (**d**) low abundance (< 10%), **e** moderate abundance (10–20%), and **f** high abundance (> 70%) of *P. cattleianum*.

structural metrics, quantifying either arrangement or heterogeneity, were derived from VAI using the R package *forestR* (Atkins and others 2018). For structural arrangement, (1) mean leaf height (m) is the average height of vegetation and (2) vertical vegetation distribution is the vertical profile of VAI through the forest column, normalized by dividing each strata height by total forest heights. For structural heterogeneity, (3) rugosity (m) is an integration of horizontal and vertical variation in VAI (Hardiman and others 2011) and (4) Gini coefficient measures the inequality of vertical vegetation distribution, from 0 (that is even VAI distribution) to 1 (maximum inequality of VAI distribution) (Gini 1912; Atkins and others 2018). Density and structural metrics were quantified for each 1 m X 6 m crosswise transect slice; For each transect, 14 slices spaced 3 m apart were averaged to ensure spatial independence (Supp. S6.1).

Structural metrics were selected for their direct relationship to forest function. The arrangement metrics, (1) leaf height and (2) vertical vegetation distribution, are linked to habitat availability and influence variation in microclimate through the forest (Vogeler and others 2013; Jucker and others 2018). The heterogeneity metrics, (3) rugosity and (4) Gini coefficient, measure horizontal and vertical complexity. Rugosity, or surface roughness, affects the thickness of the boundary air layer between forest and atmosphere, which affects forest fluxes (Baldocchi and others 2000). The Gini coefficient indicates the skew in the vertical distribution of vegetation, which affects the distribution of light and temperature in the forest (Fotis and Curtis 2017).

Statistical Analyses

To quantify differences in structural metrics (response variable) across a gradient of invasion importance value (explanatory variable), we used linear mixed effects models. We included the random effects of transect nested in site and compared three alternative specifications of the random effects: random intercepts, random slopes, and both random intercepts and random slopes (Table S2). We used an information theoretic approach to compare and evaluate models based on their explanatory power; the null model, which included

the fixed effect defined by the intercept only, was a benchmark for assessing the informative value of the other models (Bumham and Anderson 2002). The models were first fit using restricted maximum likelihood estimation and ranked by their Akaike information criterion with correction for small sample size (AICc) (Akaike 1974). The model with the lowest AICc value was considered best fit only if its ΔAICc from the model with the second lowest AICc was > 2. Second, models were fit using maximum likelihood estimation, to ensure the models were comparable despite having different fixed effects. The best-fit models were evaluated using the marginal r^2, or the variance of the fixed effects, and the conditional r^2, or the variance of both fixed and random effects (Nakagawa and Schielzeth 2013). For each best-fit model, we report the slope and intercept of the regression, indicating the fixed effect of invasion importance value (Table S3).

Biophysical Modeling

A multilayer canopy flux-profile solution described by Bonan and others (2018) for CLM-ml v0 was used to model ET. The model combined forest, soil, and climate parameters to calculate 1D fluxes of heat and energy through discretized forest strata. Radiative transfer was modeled through strata, using height-variable leaf area (derived from TLS) and leaf angles (estimated). In each stratum, the model partitions radiation into sensible and latent heat fluxes used to compute the strata's air temperature, humidity, and leaf temperature. The latter was used to calculate ET, which is constrained by strata-specific estimates of stomatal conductance. Computations occurred separately for sunlit and shaded leaf fractions, which have different specifications of stomatal conductance and leaf-absorbed radiation. Total ET, the primary model output of interest, was summed for each hour period.

Model parameters accounted for differences in soil and climate at the site-level and differences in structure at the transect-level. Parameters related to plant physiology were kept consistent between all transects and sites (Bonan 2023, Supp. S8.1). For each site, soil and climate variables were specified using December mean values for each hour from remote sensing products (Giambelluca and others 2014). For each transect, averaged VAI in each 1-m forest height strata was scaled by 0.25 to create a vertically variable estimate of *m*LAI, the model input of LAI. Stomatal conductance estimates are based on values from the TRY plant trait database for *M. polymorpha* (Kattge and others 2011). The model assumed no physiological differences between native and invasive plants for three reasons: (1) field constraints prevented direct sampling of stomatal conductance; (2) there is no evidence of statistically significant differences in leaf-level water use between *M. polymorpha* and *P. cattleianum* (Kattge and others 2011; Giambelluca 2016); and (3) parameterizing model scenarios with equivalent physiology isolates the effect of changes in forest structure on modeled evapotranspiration.

Modeling Scenario Selection

After the completion of empirical analyses of TLS measurements, modeling scenarios were designed to diagnostically measure the effect size of contrasting forest structure on ET. The scenarios isolated the impact of 1) vegetative density and 2) canopy structure independent of physiology, soil, and climate variables. Because the structural scenarios were informed by TLS measurements, modeling hypotheses were formulated after TLS analysis was complete: First, we expected increased vegetative density to increase ET. Second, we expected altered structure to influence ET independent of the changes in vegetative density.

Results

Structural Changes across the Gradient of Invasion

In the windward forest of the Island of Hawai'i, the relative abundance of invasive *P. cattleianum* had a profound impact on canopy structure across all sites. Linear mixed effects models explained variance well with fixed and random effects (high conditional r^2), but indicated large variance between sites (low marginal r^2:conditional r^2 ratio) (Table S3). According to the best-fit fixed effect model, total VAI increased 36% between native (0 IV_{inv}) and invaded (1 IV_{inv}) forest (Figure 4A, Table S3). The fixed effect model for mean leaf height projected a 3-m decrease in mean leaf height between native (0 IV_{inv}) and invaded (1 IV_{inv}) forest (Figure 4B, Table S3). The log of rugosity, which characterizes structural heterogeneity, decreased with increased IV_{inv} by 59% across the gradient of invasion (0–1 IV_{inv}; Figure 4C, Table S3). Similarly, the Gini coefficient decreased by 18% across the gradient of invasion (0–1 IV_{inv}) (Figure 4D, Table S3). The lowest Gini coefficient (0.54) corresponded with the most vertically

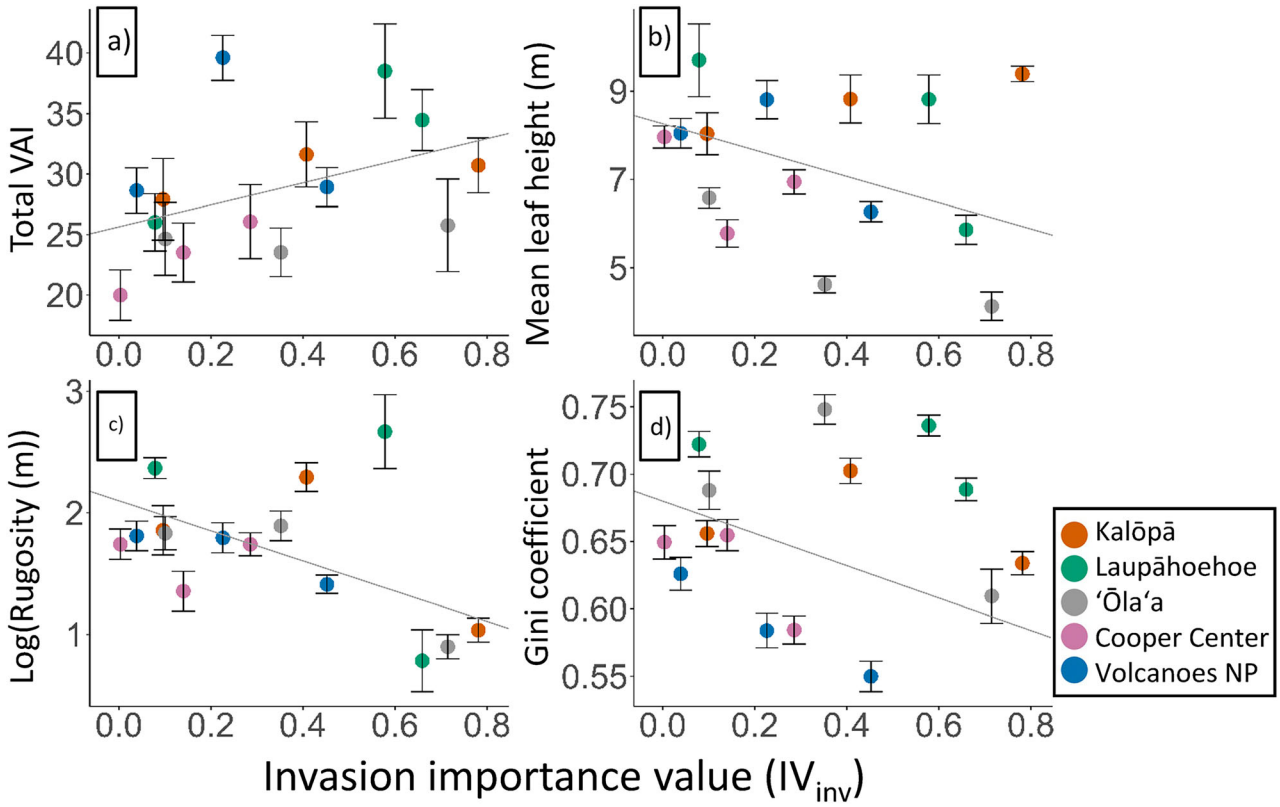


Figure 4. The response of forest density and structural metrics in Island of Hawai'i forests to *P. cattleianum* abundance, quantified as the invasion importance value (IV_{inv}). Metrics and corresponding marginal r^2 (r^2m; the variance of the fixed effects) and conditional r^2 (r^2c; the variance of both fixed and random effects) of the best-fit linear mixed effect model include **A** Total vegetation area index (VAI), ($r^2m = 0.29$; $r^2c = 0.89$); **B** Mean leaf height, ($r^2m = 0.20$; $r^2c = 0.98$); **C** Horizontal and vertical heterogeneity in vegetation distribution as measured by rugosity (natural log-transformed), ($r^2m = 0.66$; $r^2c = 0.93$); and **D** Vegetation distribution evenness as measured by the Gini coefficient, ($r^2m = 0.22$; $r^2c = 0.94$). Standard errors included. Gray lines represent the fixed effect regression line derived from the linear mixed effects model.

homogenous forest profile and was found in the Hawai'i Volcanoes National Park (hereafter, Hawai'i Volcanoes NP) invasive transect, visualized in Figure 5.

Site Specific Differences: The Vertical Distribution of Vegetation

Although total VAI increased with IV_{inv}, the vertical distribution of VAI varied by site. *P. cattleianum* invasion led to increased vegetation in different height-normalized forest strata, depending on site (Figure 5). In the site with the least amount of invasive-driven structural change (Cooper Center), invasion increased VAI with little difference in the vertical distribution of vegetation in comparison with the native-dominant transect. In the more dramatic cases of structural change, invasion increased VAI in a concentrated strata that changed the shape of VAI distribution, as in the Kalōpā invasive transect which increased vegetation in the middle forest strata compared to the Kalōpā native transect.

Modeled Evapotranspiration

The mixed and invasive transect ET_m exceeded the native transect ET_m at each site, except for the 'Ōla'a mixed and Cooper Center mixed and invasive transects (Table 2). Changes in ET_m were not directly coupled with changes in invasion gradient or changes in *m*LAI, the model input LAI. Of the three invasive/mixed transects with modeled decreases in ET_m, only the 'Ōla'a mixed transect had decreased model-scaled leaf area index (*m*LAI) compared to native transect *m*LAI. Cooper Center mixed and invasive transects had increased *m*LAI accompanied by decreased ET_m compared to the native transect. In the remaining seven mixed and invasive transects, ET_m increased with *m*LAI, but

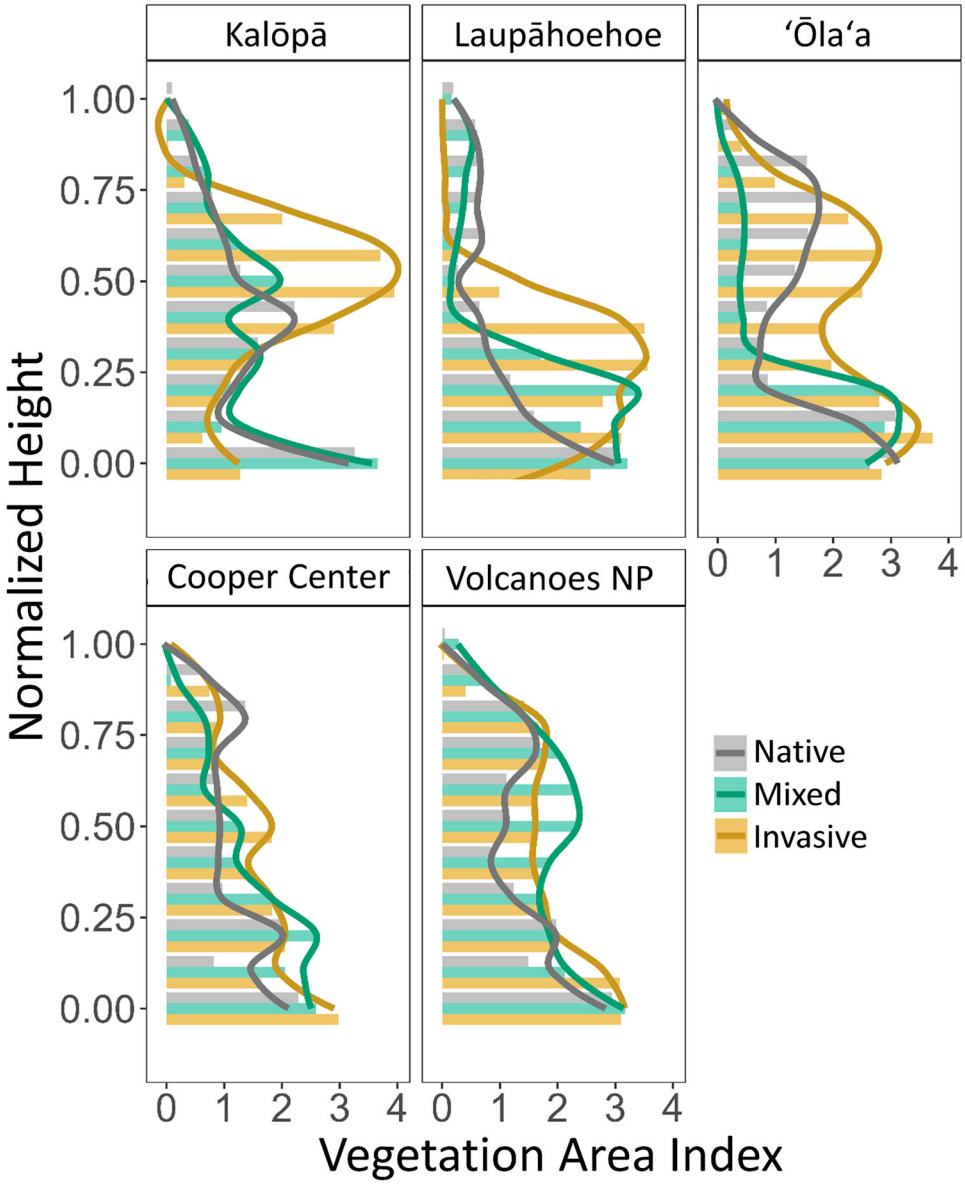


Figure 5. Vertical distribution of vegetation area index (VAI) by normalized height for native (gray), mixed (green), and invasive (gold) transects at each site. Curved lines are the locally estimated scatterplot smoothing (LOESS) regression (Cleveland 1979).

the magnitude of ET_m increase did not consistently correlate with the magnitude of *m*LAI increase. Overall, our modeled evapotranspiration (ET_m) matched remotely sensed Priestley-Taylor estimates of ET well, with an average root mean square error of ± 1.74 mm (Priestley and Taylor 1972, Table 2).

Modeling Scenarios

The modeling scenarios were designed to reflect key observed trends in vegetation amount and vertical distribution relative to a baseline ''native'' scenario, $LAI_{low}_Struct_{native}$. In Figure 6A, $LAI_{high}_Struct_{native}$ has the same relative vertical distribution of vegetation as $LAI_{low}_Struct_{native}$ but has a 1.5-fold increase in total *m*LAI (*m*LAI = 10.74) compared to $LAI_{low}_Struct_{native}$ (*m*LAI = 7.16); The 1.5-fold increase in *m*LAI increases daylight ET_m by 3.01 mm (74.0%) relative to $LAI_{low}_Struct_{native}$ ET_m (Figure 7). Scaled to 30-day estimates, this increased LAI causes a 90.2-mm increase in ET. In Figure 7B, both scenarios maintain the same ''high'' *m*LAI as $LAI_{high}_Struct_{native}$ (*m*LAI = 10.74), but vertical distribution of $LAI_{high}_Struct_{inv_mid}$ concentrates vegetation in the

Table 2. Modeled ET and LAI by Corresponding Transect Invasion Level

Site	Priestley-Taylor ET (mm)	Native		Mixed				Invasive			
		Inv. grad	ET_m (mm)	Inv. grad	ET_m (mm)	% change from native		Inv. grad	ET_m (mm)	% change from native	
						ET_m	*m*LAI			ET_m	*m*LAI
Kalōpā	3.46	0.10	3.55	0.41	4.38	23%	11.3%	0.78	7.90	123%	8.2%
Laupāhoehoe	3.30	0.08	2.59	0.58	3.88	50%	45.9%	0.66	4.53	75%	30.8%
ʻŌlaʻa	3.07	0.10	4.91	0.35	2.57	− 48%		− 4.5%	0.71	5.67	15%
4.7%											
Cooper Center	3.23	0.00	3.54	0.14	2.60	− 27%		17.6%	0.29	3.23	− 9%
30.6%											
Hawai'i Volcanoes NP	3.31	0.04	4.64	0.23	5.52	19%	38.3%	0.45	5.53	19%	1.0%

Modeled evapotranspiration (ET_m) for native, mixed, and invasive transects in each site during daylight period, hours 6–19. The percent change of modeled evapotranspiration (ET_m) and model-scaled leaf area index (mLAI) from native transect ET_m and mLAI for mixed and invasive transects demonstrates a decoupling between both variables. Priestley-Taylor ET calculated from remotely sensed climate variables is provided as a grounding measurement (Priestley and Taylor 1972).

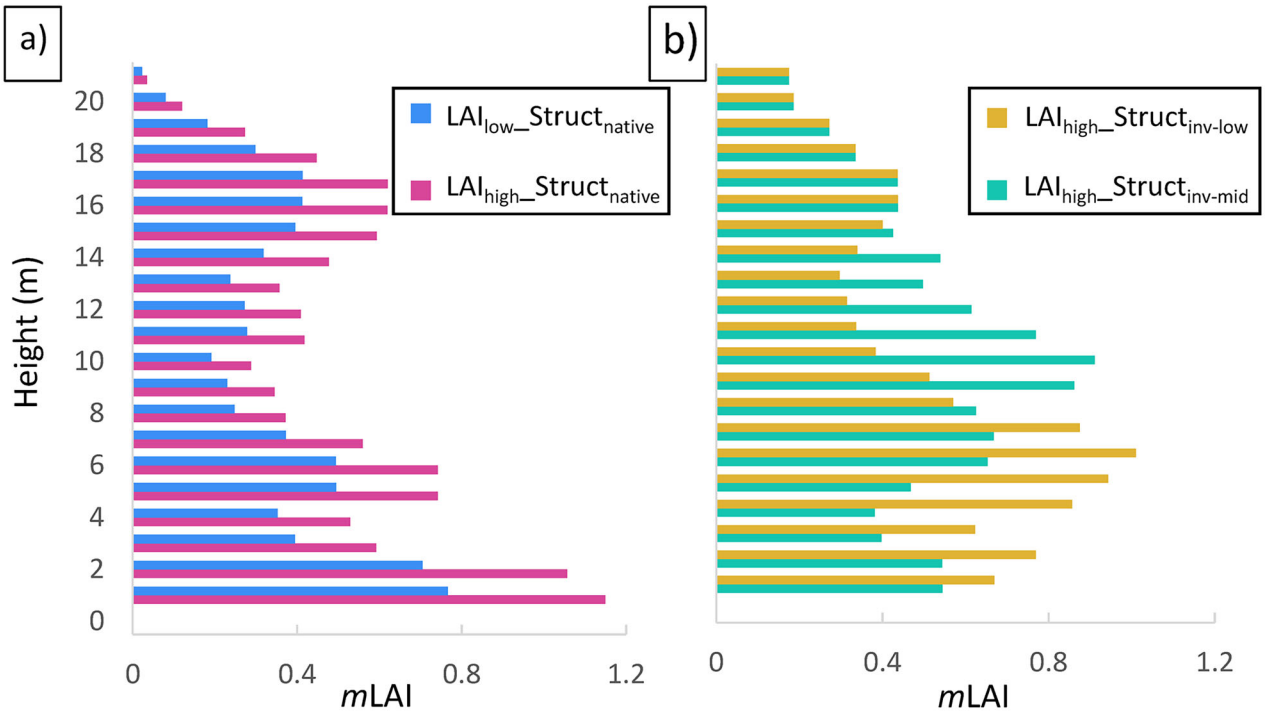


Figure 6. Vertical distribution of leaf area index used in modeling scenarios (*m*LAI). Scenario names indicate relative vegetation amount (for example 'LAI_{low}') and vegetation distribution (for example '$Struct_{native}$'). **A** In panel A, $LAI_{high}_Struct_{native}$ has the same relative vertical distribution of vegetation as $LAI_{low}_Struct_{native}$, but a 1.5-fold increase in total *m*LAI (*m*LAI = 10.74 compared to *m*LAI = 7.16). **B** In panel B, both scenarios maintain the same ''high'' *m*LAI as $LAI_{high}_Struct_{native}$ (*m*LAI = 10.74), but the vertical distribution of $LAI_{high}_Struct_{inv_mid}$ concentrates vegetation in the middle forest strata, and $LAI_{high}_Struct_{inv_low}$ concentrates vegetation in the low forest strata.

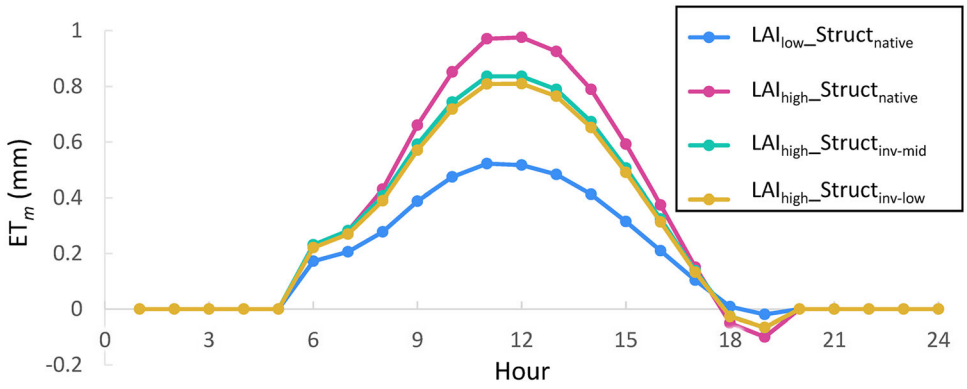


Figure 7. Modeled 24-h evapotranspiration (ET_m) for all four vegetation scenarios (Figure 6)

middle forest strata, and LAI_{high}_$Struct_{inv_low}$ concentrates vegetation in the low forest strata. Overall, differences in vegetation distribution mediated ET_m among the three model scenarios with high LAI (Figure 7): LAI_{high}_$Struct_{native}$ had the highest daytime ET_m (7.08 mm) compared to LAI_{high}_$Struct_{inv_mid}$ (6.27 mm, −11.4%) and LAI_{high}_$Struct_{inv_low}$ (6.05 mm, −14.5%). Scaled to 30-day estimates, the structural modulations in $Struct_{inv-mid}$ and $Struct_{inv-low}$ reduce 30-day ET increases due to LAI_{high} by 24.4 mm and 30.9 mm, respectively; therefore, these structural modulations could lead to differences in annual ET on the order of 100s of mm.

Discussion

Structural Impact of Invasion

The invasion of *P. cattleianum* consistently increased the density and changed the structural arrangement of vegetation in forests regardless of site-specific variation in climate, elevation, and substrate (Figure 4, Table S3). Trends such as increased VAI (density) and decreased mean leaf height (structural arrangement) matched previous studies (Asner and others 2008; Balzotti and Asner 2017). For example, the 36% increase in total VAI (density) across invasion was consistent with the 24–29% increase in LAI in invaded forest compared to native forest found in previous studies (Takahashi and others 2011; Giambelluca 2016). Although proportionally similar, VAI and LAI are difficult to directly compare because of fundamental differences in measurements: VAI represents the normalized density of LiDAR returns which includes leaves and stems (Atkins and others 2018). The 3-m decrease in mean leaf height (structural arrangement) across invasion agrees with the 3.7-m decrease in outer canopy height found in forest transitioning to *P. cattleianum* invasion over 9 years (Balzotti and Asner 2017). Takahashi and others (2011) similarly recorded a 4-m decrease in height in invaded forest compared to native *M. polymorpha*-dominant forest.

Across sites, *P. cattleianum* also had a homogenizing effect on forest structure, demonstrated by changes in (1) rugosity and (2) Gini coefficient (Figure 4C, D). (1) The decrease in rugosity with increased invasion (that is −59% from 0 to 1 IV_{inv}) aligned with Balzotti and Asner's (2017) finding that standard deviation in Laupāhoehoe's outer canopy height decreased between native and invaded forest by 28%. Decreased rugosity decreases the boundary layer turbulence at the forest-atmosphere interface, which can decrease the amount of forest ET (Baldocchi and others 2000). Although this study's vertical 1D ET model could not incorporate horizontal rugosity, conceptually, a decrease in rugosity may mitigate invasive-driven increases in ET. (2) The 18% decrease in Gini coefficient from 0 to 1 IV_{inv}, suggests invasive species homogenize the forest vertically. Vertical structural homogenization affects light attenuation and eliminates structural niches that provide important habitat (Arthur Sampson and Smith 1993; Ellison and others 2005).

Despite invasion's consistent impact to the density and structural metrics, the vertical distribution of invasive vegetation varied by site, which could be caused by several factors (Figures 1 and 4). Sites varied in climate, substrate, and elevation; such attributes' relationships to vertical distribution were not statistically tested but undoubtedly affect forest dynamics. For instance, substrate type and age, produced by gradients of past volcanic activity, are known to influence invasive and native species composition (Zimmerman and others 2008). Additionally, invasion dynamics are tightly coupled

with disturbance history (for example ungulates, disease) (Strauch and others 2016; Balzotti and Asner 2017). Within-site disturbances were assumed to be similar given transect proximity, but site variation in disturbance history was not quantified. The maturation of the *P. cattleianum* stand likely influences vertical distribution given evidence invasive trees supplant native canopy trees over time (Potter and others 2023). Similar to disturbance, site-specific differences in time since invasion could not be quantified, but a high invasion gradient and invasive vegetation approaching the canopy may indicate a relatively older *P. Cattleianum* stand age (that is, Kalōpā invaded transect, Figure 5). Longitudinal data would be required to further parse the factors driving site differences in vertical vegetation distribution.

Importance of Structural Arrangement Inferred from Modeling Scenarios

The modeling scenarios explore how structural arrangement affects ET. First, the 74% increase in ET between LAI_{high} versus LAI_{low} under equivalent vertical distribution (that is, $Struct_{native}$) represents a benchmark impact of increased LAI, absent any structural change. Theoretical and empirical analyses show ET increases with LAI, but ET increases saturate at high levels of LAI (Baldocchi and Meyers 1998). For simplicity, we use a single LAI increase benchmark, but the relative importance of structural modulation vs. LAI increase may vary depending on initial LAI. Second, modulating the structure of LAI mitigated the amount ET increased under conditions of LAI_{high}. Concentrating vegetation in the mid-forest strata (that is, $Struct_{inv\text{-}mid}$) and low-forest strata (that is $Struct_{inv\text{-}low}$), increased ET by 54% and 49%, respectively, compared to $LAI_{low}_Struct_{native}$. Essentially, structural arrangement exerts an impact on ET, secondary in magnitude to the impact of LAI on ET. These results agree with model simulations which found that ET in structurally ''top-heavy'' forest consistently exceeded ET in ''bottom-heavy'' forest with equivalent LAI, regardless of light or humidity levels (Banerjee and Linn 2018). These findings underscore the importance of incorporating vertical distribution of vegetation into assessments of forest functional changes due to invasion.

Modeling Mechanisms: Strengths and Limitations

Assumptions of equivalent stomatal conductance and net leaf radiation across sites limit the model's accuracy but strengthen its capacity to isolate the effect of site-specific structure on ET. Most importantly, the model captured the biophysical mechanism driving structural impacts on ET: leaves located higher in the canopy will be exposed to more sunlight and transpire at higher rates compared to understory leaves. Remotely sensed estimates of ET validated site-level ET*m*, but the resolution of the data (250 m^2) was too coarse to validate transect-level differences in ET*m* within each site. The model, as implemented, is more useful to explore the comparative trends of ET*m* between model simulations rather than predicting precise values of ET*m*. Still, the model's multilayer design reflects the current mechanistic understanding of radiation-driven energy fluxes and has been vetted extensively with empirical measurements (Baldocchi and others 2002; Bonan and others 2018).

Vertical gradients of canopy characteristics are notoriously undersampled due to methodological constraints (Nakamura and others 2017). In the Island of Hawai'i, we were not permitted to measure the stomatal conductance of *M. polymorpha* due to the associated risks of spreading the *Ceratocystis* sp. fungus known to cause Rapid 'Ōhi'a Death (Harrington 2013). Vertical gradients in stomatal conductance and net leaf radiation in the forest canopy are well established, but the magnitudes of the gradients vary by species and environment (Brooks and others 1997; Baldocchi and others 2002; Wittenberghe and others 2012). A limitation of the model's fixed assumptions of stomatal conductance is the inability to incorporate the ''safety-efficiency trade-off'' principle of transpiration, which states that plants maintain a maximum transpiration rate dictated by species-specific hydraulic conductivity (Manzoni and others 2013).

Functional Impact of Invasion

Modeled evapotranspiration, or ET_m, increased with invasion in 70% of mixed and invasive transects—evidence that supports the assertion that *P. cattleianum* uses more water compared to native forest (Strauch and others 2017; Table 2). However, the *P. cattleianum* invasion gradient appeared to be decoupled from ET_m: In Kalōpā, a 0.68 increase in Iv_{inv} led to 123% increase in ET_m, but in 'Ōla'a, nearly the same Iv_{inv} increase (0.61) led to just a 15% increase in ET_m. The range of ET_m increases (15–123%) exceeds previous research finding *P. cattleianum* invasion increases ET between 27 to 53% relative to native forest (Giambelluca and others, University of Hawai'i at

Mānoa, written communication, 2008). Since the model did not incorporate species-specific physiology, variation in ET_m results from the variation in vertical arrangement of vegetation (Figure 5). Structure likely mediates the relationship between invasion and ET increases, but additional empirical calibration is needed to investigate constraints on the upper bound of ET increases. In three transects with a relatively low *P. cattleianum* invasion gradient (0.14–0.35), ET_m was estimated to decrease following invasion, and only ʻŌlaʻa mixed (−48% ET_m) was accompanied by a decrease in *m*LAI (−4.5%). Under conditions of low invasion ($IV_{inv} < 0.35$), a decrease in ET may coincide with a net increase in LAI if densification of LAI occurs in the shaded understory and exceeds an accompanying reduction in canopy LAI, as observed in Cooper Center mixed and invasive transects. Therefore, although the model results support the theory that *P. cattleianum* invasion may lead to increased evapotranspiration in a heavily invaded forest, the effect on ET in sites with lower relative abundance of *P. cattleianum* is more ambiguous.

Independent of invasion level, structure influenced the nonlinear relationship observed between *m*LAI and ET_m. For example, the Kalōpā mixed transect had an 11.3% increase in *m*LAI and a 23% increase in ET_m while Kalōpā invasive transect had an 8.2% increase in *m*LAI and a 123% increase in ET_m. The structural arrangement of both transects is dramatically different, with Kalōpā invasive increasing vegetation in the middle third of the forest and Kalōpā mixed distributing increased vegetation relatively more evenly, with the exception of a spike in the 0–1-m understory strata. The comparative differences in height of *m*LAI increases explains why Kalōpā invasive had a much higher ET_m increase compared to Kalōpā mixed, despite having less overall vegetative increase. These results fit with previous research and our scenario modeling: Leppä and others (2020) found tree transpiration in a peatland forest decreased nonlinearly with decreases in forest LAI; scenario modeling highlighted the mediating role vertical vegetation distribution plays in the relationship between LAI and ET.

Management and Research Implications

Invasive species are known to reduce overall plant diversity, but invasive impacts to ecosystem function are less generalizable (McKinney and La Sorte 2007; Cavaleri and Sack 2010). Our study demonstrates that structure is an important underlying mechanism to consider when evaluating invasive-driven changes to forest function. This study highlights structural scenarios that cause the largest modeled ET increases compared to pre-invasion scenarios: heavily invaded stands ($IV_{inv} > 0.35$) in which vegetation density increases within taller, sun-exposed forest strata. Resource managers could develop plans targeting invasive stands consistent with this structural configuration to reduce impacts of *P. cattleianum* on water resources. Management approaches typically must balance multiple objectives; our study results can be used to inform management efforts aimed at mitigating impacts of invasion on ET but do not address additional forest management needs. The invasive structures we modeled were based on data from our study sites, which were limited to invasion between 0.1 to 0.8 IV_{inv} (Figure 4). Additional data describing the structure of monotypic, canopy-replacing *P. cattleianum* (that is $IV_{inv} = 1$) would be needed to represent the upward bounds of invasion (Potter and others 2023).

Additional research is needed to fully understand the impacts of *P. cattleianum* invasion on forest ET. In the state of Hawaii, area with *P. cattleianum* trees increased by 22.9% between 2010 and 2019 from 5954 to 7318 km^2 (USDA 2024). Additionally, forest disturbances can affect the pace of invasion. In particular, dieback events, Rapid ʻŌhiʻa Death, and the presence of invasive pigs create light-filled forest gaps rapidly colonized by fast-growing invasive species (Jacobi 1983; Strauch and others 2017; Fortini and others 2020). The increase in invasion area will magnify the net effect of *P. cattleianum* on the water cycle. For example, when scaled to a 25-km^2 watershed, a 4.35 mm increase in daily ET (that is, modeled in Kalōpā invasive) yields a 3.3 X 10^6 m^3 loss in water over a 30-day period. Given current pressure on water resources in Hawaii coupled with long term trends of decreasing rainfall and increasing drought, it is imperative to address invasive-driven changes to the ecohydrology of native forests (Frazier and Giambelluca 2017; Frazier and others 2022).

We identify three opportunities for additional research that could improve understanding of effects of *P. cattleianum* invasions on native forests: resolving species-specific physiology, scaling the modeling, and exploring other forest variables. First, *P. cattleianum* is theorized to have higher demand for water than native species, but results to date do not confirm significant differences in leaf-level water use (Kattge and others 2011; Giambelluca 2016). Our work demonstrates that structural differences due to invasion lead to changes in ET independent of physiological differences. However,

physiological differences, such as differences in hydraulic conductivity, can impose constraints on plant transpiration (Manzoni and others 2013). Research verifying physiological differences in water use between species could improve model parameterization and yield more insightful results. Second, this study's multilayer canopy model approximates only the vertical flux of water and energy, and ET was validated at the site, rather than transect, level. Empirical measurements of ET that match the fine spatial scale of the model are required to quantify model uncertainty. Additionally, a 3D model could scale results to the watershed level and incorporate invasive impacts to the boundary layer. Finally, this study ecologically simplifies *P. cattleianum* as the main competitor to *M. polymorpha*. In many cases, forest stands on the Island of Hawai'i are invaded by multiple invasive species which are likely to affect forest function and alter inter-species interactions (Hughes and Denslow 2005). More accurately capturing the diversity in functional and structural complexity could improve model results.

ACKNOWLEDGEMENTS

The authors are grateful to Josie Tupu and Christina Leopold for their support and assistance. We appreciate the financial support from the National Science Foundation, the Rudy Grah Endowed Chair in Forestry and Sustainability, and the Hannah M. and Frank Schwabacher Memorial Scholarship Fund. Logistic support was provided by the U.S. Geological Survey and the National Park Service. Any use of trade, firm, or product names is for descriptive purposes only and does not imply endorsement by the U.S. Government.

FUNDING

Rudy Grah Endowed Chair in Forestry and Sustainability, Hannah M. and Frank Schwabacher Memorial Scholarship Fund, National Science Foundation, Graduate Research Fellowship Program, Graduate Research Internship Program.

DATA AVAILABILITY

Data are accessible in a Dryad repository. The structural and functional impacts of invasive *Psidium cattleianum* in forests on the Island of Hawai'i https://doi.org/10.5061/dryad.80gb5mm1g.

OPEN ACCESS

This article is licensed under a Creative Commons Attribution 4.0 International License, which permits use, sharing, adaptation, distribution and reproduction in any medium or format, as long as you give appropriate credit to the original author(s) and the source, provide a link to the Creative Commons licence, and indicate if changes were made. The images or other third party material in this article are included in the article's Creative Commons licence, unless indicated otherwise in a credit line to the material. If material is not included in the article's Creative Commons licence and your intended use is not permitted by statutory regulation or exceeds the permitted use, you will need to obtain permission directly from the copyright holder. To view a copy of this licence, visit http://creativecommons.org/licenses/by/4.0/.

REFERENCES

Adee K, Conrad E. 1990. Metrosideros polymorpha Gaud. 'Ohi'a lehua. In: Silvics of North America: conifers, Vol. 2. Agriculture handbook. Washington, DC: U.S. Department of Agriculture, Forest Service. pp 466–9.

Akaike H. 1974. A new look at the statistical model identification. IEEE Trans Autom Control 19:716–723.

Arthur Sampson D, Smith FW. 1993. Influence of canopy architecture on light penetration in lodgepole pine (*Pinus contorta* var. latifolia) forests. Agric for Meteorol 64:63–79.

Asner GP, Hughes RF, Vitousek PM, Knapp DE, Kennedy-Bowdoin T, Boardman J, Martin RE, Eastwood M, Green RO. 2008. Invasive plants transform the three-dimensional structure of rain forests. In: Proceedings of the National Academy of Sciences105:4519–23.

Atkins JW, Bohrer G, Fahey RT, Hardiman BS, Morin TH, Stovall AEL, Zimmerman N, Gough CM. 2018. Quantifying vegetation and canopy structural complexity from terrestrial LiDAR data using the forestr r package. Methods Ecol Evol 9:2057–2066.

Baldocchi D, Meyers T. 1998. On using eco-physiological, micrometeorological and biogeochemical theory to evaluate carbon dioxide, water vapor and trace gas fluxes over vegetation: a perspective. Agric for Meteorol 90:1–25.

Baldocchi D, Finnigan J, Wilson K, Paw UKT, Falge E. 2000. On measuring net ecosystem carbon exchange over tall vegetation on complex terrain. Bound-Layer Meteorol 96:257–291.

Baldocchi DD, Wilson KB, Gu L. 2002. How the environment, canopy structure and canopy physiological functioning influence carbon, water and energy fluxes of a temperate broad-leaved deciduous forest—an assessment with the biophysical model CANOAK. Tree Physiol 22:1065–1077.

Balzotti CS, Asner GP. 2017. Episodic canopy structural transformations and biological invasion in a Hawaiian Forest. Front Plant Sci 8:1256.

Banerjee T, Linn R. 2018. Effect of vertical canopy architecture on transpiration, thermoregulation and carbon assimilation. Forests 9:198.

Becker P, Nichols T. 2011. Effects of basal area factor and plot size on precision and accuracy of forest inventory estimates. North J Appl for 28:152–156.

Béland M, Baldocchi DD. 2021. Vertical structure heterogeneity in broadleaf forests: effects on light interception and canopy photosynthesis. Agric for Meteorol 307:108525.

Béland M, Parker G, Sparrow B, Harding D, Chasmer L, Phinn S, Antonarakis A, Strahler A. 2019. On promoting the use of lidar systems in forest ecosystem research. For Ecol Manag 450:117484.

Bonan G. 2019. Climate Change and Terrestrial Ecosystem Modeling. Cambridge: Cambridge University Press.

Bonan GB, Patton EG, Harman IN, Oleson KW, Finnigan JJ, Lu Y, Burakowski EA. 2018. Modeling canopy-induced turbulence in the Earth system: a unified parameterization of turbulent exchange within plant canopies and the roughness sublayer (CLM-ml v0). Geosci Model Dev 11:1467–1496.

Bonan GB, Patton EG, Finnigan JJ, Baldocchi DD, Harman IN. 2021. Moving beyond the incorrect but useful paradigm: reevaluating big-leaf and multilayer plant canopies to model biosphere-atmosphere fluxes – a review. Agric for Meteorol 306:108435.

Bonan G. 2023. Matlab Code for Climate Change and Terrestrial Ecosystem Modeling. https://github.com/gbonan/bonanmodeling. Last Accessed 11 Oct 2022.

Bonham CD. 2013. Measurements for Terrestrial Vegetation. John Wiley & Sons.

Brooks JR, Flanagan LB, Varney GT, Ehleringer JR. 1997. Vertical gradients in photosynthetic gas exchange characteristics and refixation of respired CO2 within boreal forest canopies. Tree Physiol 17:1–12.

Buckley DS, Isebrands JG, Sharik TL. 1999. Practical field methods of estimating canopy cover, PAR, and LAI in Michigan Oak and Pine Stands. North J Appl for 16:25–32.

Bumham KP, Anderson DR. 2002. Model selection and multimodel inference: a practical information-theoretic approach. New York, New York: Spnnger-Veflag https://cir.nii.ac.jp/crid/1572543026243620608. Last Accessed 21 Feb 2025

Calder IR, Dye P, editors. 2001. Hydrological impacts of invasive alien plants. Land Use Water Resour Res.

Cavaleri MA, Sack L. 2010. Comparative water use of native and invasive plants at multiple scales: a global meta-analysis. Ecology 91:2705–2715.

Cavaleri MA, Ostertag R, Cordell S, Sack L. 2014. Native trees show conservative water use relative to invasive trees: results from a removal experiment in a Hawaiian wet forest. Conserv Physiol 2:cou016.

Cleveland WS. 1979. Robust locally weighted regression and smoothing scatterplots. J Am Stat Assoc 74:829–836.

D'Antonio CM, Vitousek PM. 1992. Biological invasions by exotic grasses, the grass/fire cycle, and global change. Annu Rev Ecol Syst 23:63–87.

de Almeida DRA, Stark SC, Shao G, Schietti J, Nelson BW, Silva CA, Gorgens EB, Valbuena R, de Almeida Papa D, Brancalion PHS. 2019. Optimizing the remote detection of tropical rainforest structure with airborne lidar: leaf area profile sensitivity to pulse density and spatial sampling. Remote Sens 11:1–15.

De Frenne P, Lenoir J, Luoto M, Scheffers BR, Zellweger F, Aalto J, Ashcroft MB, Christiansen DM, Decocq G, De Pauw K, Govaert S, Greiser C, Gril E, Hampe A, Jucker T, Klinges DH, Koelemeijer IA, Lembrechts JJ, Marrec R, Meeussen C, Ogée J, Tyystjärvi V, Vangansbeke P, Hylander K. 2021. Forest microclimates and climate change: importance, drivers and future research agenda. Glob Change Biol 27:2279–2297.

Denslow JS. 2003. Weeds in paradise: thoughts on the invasibility of tropical islands. Ann Mo Bot Gard 90:119–127.

Ehrenfeld JG. 2010. Ecosystem consequences of biological invasions. Annu Rev Ecol Evol Syst 41:59–80.

Ellison AM, Bank MS, Clinton BD, Colburn EA, Elliott K, Ford CR, Foster DR, Kloeppel BD, Knoepp JD, Lovett GM, Mohan J, Orwig DA, Rodenhouse NL, Sobczak WV, Stinson KA, Stone JK, Swan CM, Thompson J, Von Holle B, Webster JR. 2005. Loss of foundation species: consequences for the structure and dynamics of forested ecosystems. Front Ecol Environ 3:479–486.

Esri, Maxar, Earthstar Geographics, GIS User Community. 2025. World Imagery. https://doc.arcgis.com/en/data-appliance/latest/maps/world-imagery.htm

Fortini LB, Leopold C, Perkins K, Chadwick O, Yelenik S, Jacobi J, Bishaw KI, Gregg M, Rosa S. 2020. Local to landscape-level controls of water fluxes through Hawaiian forests: Effects of invasive animals and plants on soil infiltration capacity across substrate and moisture gradients. http://hdl.handle.net/10790/5282. Last Accessed 11 Oct 2023

Fotis AT, Curtis PS. 2017. Effects of structural complexity on within-canopy light environments and leaf traits in a northern mixed deciduous forest. Tree Physiol 37:1426–1435.

Frazier AG, Giambelluca TW. 2017. Spatial trend analysis of Hawaiian rainfall from 1920 to 2012. Int J Climatol 37:2522–2531.

Frazier AG, Giardina CP, Giambelluca TW, Brewington L, Chen Y-L, Chu P-S, Berio Fortini L, Hall D, Helweg DA, Keener VW, Longman RJ, Lucas MP, Mair A, Oki DS, Reyes JJ, Yelenik SG, Trauernicht C. 2022. A century of drought in Hawai'i: geospatial analysis and synthesis across hydrological, ecological, and socioeconomic scales. Sustainability 14:12023.

Giambelluca TW. 2002. Hydrology of altered tropical forest. Hydrol Process 16:1665–1669.

Giambelluca TW, Delay JK, Asner GP, Martin RE, Nullet MA, Huang M, Mudd RG, Takahashi M. 2008. Stand structural controls on evapotranspiration in native and invaded tropical montane cloud forest in Hawai'i. In AGU fall meeting abstracts 2008:B43A–0422.

Giambelluca TW, Chen Q, Frazier AG, Price JP, Chen Y-L, Chu P-S, Eischeid JK, Delparte DM. 2013. Online rainfall atlas of Hawai'i. Bull Am Meteorol Soc 94:313–316.

Giambelluca TW, Shuai X, Barnes ML, Alliss RJ, Longman RJ, Miura T, Chen Q, Frazier AG, Mudd RG, Cuo L, Businger AD. 2014. Evapotranspiration of Hawai'i Final Report. U.S. Army Corps of Engineers - Honolulu District and Commission on Water Resource Management, State of Hawai'i

Giambelluca T. 2016. Final Report: Understanding the Response of Native and Non-native Forests to Climate Variability and Change to Support Resource Management in Hawai'i. University of Hawai'i Mānoa https://www.sciencebase.gov/catalog/item/5876c02de4b0aa226e1c8143. Last Accessed 13 Feb 2023

Gini C. 1912. Variabilità e Mutuabilità: contributo allo studio delle distribuzioni e delle relazioni statistiche. Bologna: Tipogr. di P. Cuppini.

Hardiman BS, Bohrer G, Gough CM, Vogel CS, Curtis PS. 2011. The role of canopy structural complexity in wood net primary production of a maturing northern deciduous forest. Ecology 92:1818–1827.

Harrington TC. 2013. Ceratocystis diseases. In: Gonthier P, Nicolotti G, editors. Infectious forest diseases. 1st ed. UK: CABI. pp 230–55. http://www.cabidigitallibrary.org. https://doi.org/10.1079/9781780640402.0230. Last accessed 02/10/2023

Hawaii statewide GIS program. 2021. Hawaii DTM. <https://geoportal.hawaii.gov/datasets/HiStateGIS::hawaii-dtm-elevation/about>

Hughes RF, Denslow JS. 2005. Invasion by a N2-fixing tree alters function and structure in Wet Lowland Forests of Hawaii. Ecol Appl 15:1615–1628.

Jacobi JD. 1983. Metrosideros dieback in Hawai'i: a comparison of adjacent dieback and non-dieback rain forest stands. N Z J Ecol 6:79–97.

Jucker T, Hardwick SR, Both S, Elias DMO, Ewers RM, Milodowski DT, Swinfield T, Coomes DA. 2018. Canopy structure and topography jointly constrain the microclimate of human-modified tropical landscapes. Glob Change Biol 24:5243–5258.

Kattge J, Díaz S, Lavorel S, Prentice IC, Leadley P, Bönisch G, Garnier E, Westoby M, Reich PB, Wright IJ, Cornelissen JHC, Violle C, Harrison SP, Van BODEGOMPM, Reichstein M, Enquist BJ, Soudzilovskaia NA, Ackerly DD, Anand M, Atkin O, Bahn M, Baker TR, Baldocchi D, Bekker R, Blanco CC, Blonder B, Bond WJ, Bradstock R, Bunker DE, Casanoves F, Cavender-Bares J, Chambers JQ, Chapin Iii FS, Chave J, Coomes D, Cornwell WK, Craine JM, Dobrin BH, Duarte L, Durka W, Elser J, Esser G, Estiarte M, Fagan WF, Fang J, Fernández-Méndez F, Fidelis A, Finegan B, Flores O, Ford H, Frank D, Freschet GT, Fyllas NM, Gallagher RV, Green WA, Gutierrez AG, Hickler T, Higgins SI, Hodgson JG, Jalili A, Jansen S, Joly CA, Kerkhoff AJ, Kirkup D, Kitajima K, Kleyer M, Klotz S, Knops JMH, Kramer K, Kühn I, Kurokawa H, Laughlin D, Lee TD, Leishman M, Lens F, Lenz T, Lewis SL, Lloyd J, Llusià J, Louault F, Ma S, Mahecha MD, Manning P, Massad T, Medlyn BE, Messier J, Moles AT, Müller SC, Nadrowski K, Naeem S, Niinemets Ü, Nöllert S, Nüske A, Ogaya R, Oleksyn J, Onipchenko VG, Onoda Y, Ordoñez J, et al. 2011. TRY – a global database of plant traits. Glob Change Biol 17:2905–2935.

König C, Weigelt P, Taylor A, Stein A, Dawson W, Essl F, Pergl J, Pyšek P, van Kleunen M, Winter M, Chatelain C, Wieringa JJ, Krestov P, Kreft H. 2021. Disharmony of the world's island floras. Ecography 44:44–55.

Leppä K, Korkiakoski M, Nieminen M, Laiho R, Hotanen J-P, Kieloaho A-J, Korpela L, Laurila T, Lohila A, Minkkinen K, Mäkipää R, Ojanen P, Pearson M, Penttilä T, Tuovinen J-P, Launiainen S. 2020. Vegetation controls of water and energy balance of a drained peatland forest: responses to alternative harvesting practices. Agric for Meteorol 295:108198.

Mair A, Fares A. 2010. Throughfall characteristics in three non-native Hawaiian forest stands. Agric for Meteorol 150:1453–1466.

Manzoni S, Vico G, Katul G, Palmroth S, Jackson RB, Porporato A. 2013. Hydraulic limits on maximum plant transpiration and the emergence of the safety–efficiency trade-off. New Phytol 198:169–178.

McGeoch MA, Butchart SHM, Spear D, Marais E, Kleynhans EJ, Symes A, Chanson J, Hoffmann M. 2010. Global indicators of biological invasion: species numbers, biodiversity impact and policy responses. Divers Distrib 16:95–108.

McKinney ML, La Sorte FA. 2007. Invasiveness and homogenization: synergism of wide dispersal and high local abundance. Glob Ecol Biogeogr 16:394–400.

Murphy BA, May JA, Butterworth BJ, Andresen CG, Desai AR. 2022. Unraveling forest complexity: resource use efficiency, disturbance, and the structure-function relationship. J Geophys Res Biogeosci 127:e2021JG006748.

Nakagawa S, Schielzeth H. 2013. A general and simple method for obtaining R2 from generalized linear mixed-effects models. Methods Ecol Evol 4:133–142.

Nakamura A, Kitching RL, Cao M, Creedy TJ, Fayle TM, Freiberg M, Hewitt CN, Itioka T, Koh LP, Ma K, Malhi Y, Mitchell A, Novotny V, Ozanne CMP, Song L, Wang H, Ashton LA. 2017. Forests and their canopies: achievements and horizons in Canopy science. Trends Ecol Evol 32:438–451.

Ostertag R, Cordell S, Michaud J, Cole TC, Schulten JR, Publico KM, Enoka JH. 2009. Ecosystem and restoration consequences of invasive woody species removal in Hawaiian lowland wet forest. Ecosystems 12:503–515.

Pejchar L, Mooney HA. 2009. Invasive species, ecosystem services and human well-being. Trends Ecol Evol 24:497–504.

Potter KM, Giardina C, Hughes RF, Cordell S, Kuegler O, Koch A, Yuen E. 2023. How invaded are Hawaiian forests? Non-native understory tree dominance signals potential canopy replacement. Landsc Ecol. https://doi.org/10.1007/s10980-023-01662-6.

Priestley CHB, Taylor RJ. 1972. On the Assessment of Surface Heat Flux and Evaporation Using Large-Scale Parameters. https://journals.ametsoc.org/view/journals/mwre/100/2/1520-0493_1972_100_0081_otaosh_2_3_co_2.xml. Last Accessed 19 Jan 2025

Pyšek P, Richardson DM. 2010. Invasive species, environmental change and management, and health. Annu Rev Environ Resour 35:25–55.

Pyšek P, Jarošík V, Hulme PE, Pergl J, Hejda M, Schaffner U, Vilà M. 2012. A global assessment of invasive plant impacts on resident species, communities and ecosystems: the interaction of impact measures, invading species' traits and environment. Glob Change Biol 18:1725–1737.

Reaser JK, Meyerson LA, Cronk Q, Poorter MD, Eldrege LG, Green E, Kairo M, Latasi P, Mack RN, Mauremootoo J, O'dowd D, Orapa W, Sastroutomo S, Saunders A, Shine C, Thrainsson S, Vaiutu L. 2007. Ecological and socioeconomic impacts of invasive alien species in island ecosystems. Environ Conserv 34:98–111.

Rojas-Sandoval J, Ackerman JD, Marcano-Vega H, Willig MR. 2022. Alien species affect the abundance and richness of native species in tropical forests: the role of adaptive strategies. Ecosphere 13:e4291.

Safeeq M, Fares A. 2012. Hydrologic response of a Hawaiian watershed to future climate change scenarios. Hydrol Process 26:2745–2764.

Seebens H, Blackburn TM, Dyer EE, Genovesi P, Hulme PE, Jeschke JM, Pagad S, Pyšek P, Winter M, Arianoutsou M, Bacher S, Blasius B, Brundu G, Capinha C, Celesti-Grapow L, Dawson W, Dullinger S, Fuentes N, Jäger H, Kartesz J, Kenis M, Kreft H, Kühn I, Lenzner B, Liebhold A, Mosena A, Moser D, Nishino M, Pearman D, Pergl J, Rabitsch W, Rojas-Sandoval J, Roques A, Rorke S, Rossinelli S, Roy HE, Scalera R, Schindler S, Štajerová K, Tokarska-Guzik B, van Kleunen M, Walker K, Weigelt P, Yamanaka T, Essl F. 2017. No saturation in the accumulation of alien species worldwide. Nat Commun 8:14435.

Sherrod DR, Robinson JE, Sinton JM, Watkins SE, Brunt KM. 2021. Geologic map database to accompany geologic map of the State of Hawai: U.S. Geological Survey data release. h

ttps://www.sciencebase.gov/catalog/item/60df56d5d34ed15aa3b8a39c

Stark SC, Breshears DD, Aragón S, Villegas JC, Law DJ, Smith MN, Minor DM, de Assis RL, de Almeida DRA, de Oliveira G, Saleska SR, Swann ALS, Moura JMS, Camargo JL, da Silva R, Aragão LEOC, Oliveira RC. 2020. Reframing tropical savannization: linking changes in canopy structure to energy balance alterations that impact climate. Ecosphere 11:e03231.

Strauch AM, Bruland GL, MacKenzie RA, Giardina CP. 2016. Soil and hydrological responses to wild pig (*Sus scofa*) exclusion from native and strawberry guava (*Psidium cattleianum*)-invaded tropical montane wet forests. Geoderma 279:53–60.

Strauch AM, Giardina CP, MacKenzie RA, Heider C, Giambelluca TW, Salminen E, Bruland GL. 2017. Modeled effects of climate change and plant invasion on watershed function across a steep tropical rainfall gradient. Ecosystems 20:583–600.

Takahashi M, Giambelluca TW, Mudd RG, DeLay JK, Nullet MA, Asner GP. 2011. Rainfall partitioning and cloud water interception in native forest and invaded forest in Hawai'i Volcanoes National Park. Hydrol Process 25:448–464.

U.S. Geological Survey (USGS). 2015. USGS 10-m Digital Elevation Model (DEM): Hawaii: Big Island. http://pacioos.org/metadata/usgs_dem_10m_bigisland.html

USDA. 2024. Forest Inventory and Analysis Data Mart. https://apps.fs.usda.gov/fia/datamart/datamart.html

van Kleunen M, Dawson W, Essl F, Pergl J, Winter M, Weber E, Kreft H, Weigelt P, Kartesz J, Nishino M, Antonova LA, Barcelona JF, Cabezas FJ, Cárdenas D, Cárdenas-Toro J, Castaño N, Chacón E, Chatelain C, Ebel AL, Figueiredo E, Fuentes N, Groom QJ, Henderson L, Inderjit Kupriyanov A, Masciadri S, Meerman J, Morozova O, Moser D, Nickrent DL, Patzelt A, Pelser PB, Baptiste MP, Poopath M, Schulze M, Seebens H, Shu W, Thomas J, Velayos M, Wieringa JJ, Pyšek P. 2015. Global exchange and accumulation of non-native plants. Nature 525:100–103.

Van Wittenberghe S, Adriaenssens S, Staelens J, Verheyen K, Samson R. 2012. Variability of stomatal conductance, leaf anatomy, and seasonal leaf wettability of young and adult European beech leaves along a vertical canopy gradient. Trees 26:1427–1438.

Vilà M, Espinar JL, Hejda M, Hulme PE, Jarošík V, Maron JL, Pergl J, Schaffner U, Sun Y, Pyšek P. 2011. Ecological impacts of invasive alien plants: a meta-analysis of their effects on species, communities and ecosystems. Ecol Lett 14:702–708.

Vitousek PM, Walker LR, Whiteaker LD, Mueller-Dombois D, Matson PA. 1987. Biological invasion by *Myrica faya* alters ecosystem development in Hawaii. Science 238:802–804.

Vogeler JC, Hudak AT, Vierling LA, Vierling KT. 2013. Lidar-derived canopy architecture predicts brown creeper occupancy of two western coniferous forests. The Condor 115:614–622.

Wensel LC, Levitan J, Barber K. 1980. Selection of Basal area factor in point sampling. J for 78:83–84.

Zimmerman N, Flint Hughes R, Cordell S, Hart P, Chang HK, Perez D, Like RK, Ostertag R. 2008. Patterns of primary succession of native and introduced plants in lowland wet forests in Eastern Hawai'i. Biotropica 40:277–284.